Antiferromagnetism, structural properties, and electronic transport of $BaCo_{0.9}Ni_{0.1}S_{1.8}$

S. A. M. Mentink* and T. E. Mason
Department of Physics, University of Toronto, 60 Saint George Street, Toronto, Ontario, Canada M5S 1A7

B. Fisher, J. Genossar, L. Patlagan, and A. Kanigel
Department of Physics and Crown Center for Superconductivity, Technion, Haifa, Israel 32000

M. D. Lumsden and B. D. Gaulin
Department of Physics and Astronomy and the Brockhouse Institute for Materials Research, McMaster University, Hamilton, Ontario, Canada L8S 4M1

(Received 8 August 1996; revised manuscript received 6 February 1997)

The layered transition-metal compound $BaCo_{0.9}Ni_{0.1}S_{1.8}$ is an antiferromagnetic insulator, $T_N = 280$ K, which undergoes a unique insulator to metal transition at $T_s = 200$ K. By x-ray and neutron powder diffraction we explore the difference in crystal structure above and below T_s. The magnetic structure consists of Co moments of $1.8 \pm 0.5\ \mu_B$ with antiferromagnetic nearest-neighbor interactions. Below T_s long-range order disappears. Resistivity and thermoelectric power measurements indicate that above T_s this system is a narrow-band material with dominating nearest-neighbor hopping. Magnetoresistance to 12 T shows insensitivity of T_s to magnetic fields. The length changes at T_s as measured by dilatometry are much larger than for ordinary first-order phase transitions. [S0163-1829(97)06118-3]

I. INTRODUCTION

First-order phase transitions from a low-temperature paramagnetic metal (PMM) to a high-temperature antiferromagnetic insulator (AFI) are very unusual. Recently, such a transition was reported in the alloy system $BaCo_{1-x}Ni_xS_{2-y}$ (BaCoNiS) in the composition range $0.05 \leqslant x \leqslant 0.20$ and $0.05 \leqslant y \leqslant 0.20$.[1] These alloys are layered tetragonal transition-metal sulfides[2] with structural characteristics analogous to the high-T_c superconducting oxides. The transition (with transition temperature T_s) occurs in an antiferromagnetic state and is accompanied by a lowering of crystallographic symmetry. This remarkable AFI-PMM transition in BaCoNiS could prove to be one of the few examples supporting the model of *resonant pinning* in layered compounds with metal-semiconductor components, put forward by Phillips[3] in an attempt to describe the high-T_c superconductors. According to this model a large peak in the density of electronic states at E_F, associated with the anion dopants from the oxygen column in the periodic table, may be stabilized by an *anti-Jahn-Teller* effect, as energy may be gained by improved screening of long-range ionic potentials. The recently reported pressure dependence of T_s is consistent with such a model.[4]

The parent material of the alloy under investigation, orthorhombic $BaCoS_2$, is regarded as a Mott insulator.[5,6] It has a Néel temperature, T_N, very close to room temperature (RT).[5] Around RT its resistivity, $\rho(T)$, is thermally activated with an activation energy of $\Delta \simeq 0.17$ eV. In the antiferromagnetic state, below ~ 250 K, $\ln\rho$ vs T^{-1} exhibits a curvature that implies a decrease of Δ with decreasing temperature.[5] The substitution of several percent of nickel for cobalt in $BaCoS_2$ stabilizes the tetragonal structure of $BaNiS_2$. The lattice constants decrease with increasing x; the unit-cell volume of $BaCoS_2$ is 7.2% larger than that of metallic $BaNiS_2$. Upon increasing x in $BaCo_{1-x}Ni_xS_2$, T_N gradually decreases and an antiferromagnetic insulator to paramagnetic metal (AFI-PMM) transition occurs.[1,7] The temperature coefficient of the resistivity becomes positive at all temperatures for $x \geqslant 0.25$. For a range of nickel concentrations, the transport and magnetic properties of $BaCo_{1-x}Ni_xS_2$ resemble those of the cuprate superconductors in their normal state.[7]

Sulfur depletion in $BaCo_{0.9}Ni_{0.1}S_{2-y}$ raises T_N, the RT resistivity and its activation energy; hence the sulfur vacancies compensate for the effect of nickel doping. The RT lattice constants do not change. At lower temperatures, these vacancies induce the very unusual and dramatic AFI-PMM transition at T_s.[1] The largest resistivity ratio going from the insulating (I) to the metallic (M) phase, $\rho_I/\rho_M > 10^3$, was found in samples with $x = 0.1$ and $y = 0.2$ at $T_s \simeq 200$ K. For $x = 0.1$ and $y < 0.2$, ρ_I/ρ_M decreases, while the width of the hysteresis increases.

The magnetic susceptibility, $\chi(T)$, exhibits a sharp drop upon cooling through T_s. It is noteworthy that although the resistivity jump depends strongly on y, the change in susceptibility is almost the same for $y = 0.1$, 0.15, and 0.2.[1] Recently, application of hydrostatic pressure was observed by Looney *et al.*,[4] to depress T_s on heating and cooling. Using the Clausius-Clapeyron equation and the measured dT_s/dp, these authors calculated an entropy change of 0.6 cal/mole K at the transition of a sample with $x = y = 0.1$. A similar value was obtained from specific-heat measurements on a sample with the same nominal composition.[8]

Here we use x-ray-diffraction measurements to assess the structural change at T_s from tetragonal to, possibly, orthorhombic symmetry. Powder neutron diffraction is used to investigate the type of antiferromagnetic order in $BaCo_{0.9}Ni_{0.1}S_{1.8}$ and its role in the AFI-PMM transition. Resistivity measurements in zero and magnetic fields up to 12 T

are used to derive the temperature dependence of the activation energy in the insulating phase and to study the influence of a magnetic field on T_s and T_N. Thermoelectric power measurements show the narrow-band character of this material. Finally, we performed dilatometry in the vicinity of T_s and find unusually large length changes, one to two orders of magnitude larger than associated with ordinary first-order phase transitions.

This paper is organized as follows: after briefly describing sample preparation and the employed experimental techniques in Sec. II, we discuss the structural properties of $BaCo_{0.9}Ni_{0.1}S_{1.8}$ above and below T_s in Sec. III A. Section III B describes the antiferromagnetic ordering and its temperature evolution. In Sec. IV resistivity, thermoelectric power, and thermal-expansion experiments are presented. Finally, we present a summary of our results and their interpretation in Sec. V.

II. SAMPLE PREPARATION AND EXPERIMENTAL TECHNIQUES

We prepared polycrystalline samples of $BaCo_{1-x}Ni_xS_{2-y}$ with nominal composition $x = 0.1$ and $y = 0.2$, aiming at the composition that showed the highest resistivity ratio at the AFI-PMM transition as reported in Ref. 1. The preparation procedure was essentially the same as described in Ref. 1 and need not be restated here. We varied the temperature of the last anneal and found that the optimal annealing temperature for obtaining samples with highest resistivity ratio was around 880–890 °C. The size of the resistivity jump for our best sample, also used in the x-ray measurements, is the same as for $y = 0.15$ in Ref. 1. For our sample studied by neutron diffraction the jump is smaller, but comparable to that observed at ambient pressure by Looney *et al.*[4] We caution the reader that the samples under investigation by various groups, and the different samples studied here, have slightly differing compositions, transition temperatures, and resistivity jumps. It is possible that small fractions of a sample do not undergo a structural transition due to a different stoichiometry than the main phase. These effects have little influence on the following discussion, but will be referred to when necessary.

High-resolution powder x-ray-diffraction measurements were carried out on a powder sample of $BaCo_{0.9}Ni_{0.1}S_{1.8}$, sintered at 890 °C. Measurements were made with an 18 kW Rigaku rotating anode x-ray generator and a double-axis diffractometer using a flat pyrolytic graphite (0 0 2) monochromator which selected Cu K_α radiation, $\lambda = 1.54178$ Å. Four sets of slit assemblies, two in both incident and scattered beam, allowed control of the resolution. The bulk sample was glued to the cold finger of a Displex closed-cycle helium refrigerator with Be windows. In this manner a temperature range from 20–300 K was covered. Neutron-diffraction experiments were performed at the DUALSPEC high-resolution diffractometer at the NRU reactor of AECL Research, Chalk River. Approximately 6 g of similarly prepared sample was powdered in a He atmosphere and sealed in a vanadium container filled with He-exchange gas. The neutron wavelength was 1.5048 Å. Full diffractograms ($5° < 2\Theta < 120°$) were recorded at 4.7, 147, and 290 K, while a smaller 2Θ range of 5–80° was measured while varying temperature through T_N and T_s. The resistance of the samples was measured using an *ac* four-probe method in a standard ^{4}He cryostat in magnetic fields up to 12 T. The thermoelectric power measurements were performed in a cryostat operating from 77 to 400 K. Finally, the length changes of several samples were determined as function of temperature, both on heating and cooling, using a capacitor dilatometer.

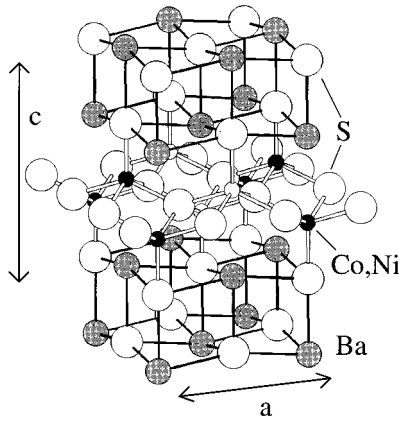

FIG. 1. Crystal structure of $BaCo_{0.9}Ni_{0.1}S_{1.8}$, with orthorhombic lattice parameters a ($b \sim a$) and c. Note the presence of a double layer of Co-S, with monolayers at distance $z = 0.18c \simeq 1.6$ Å. The magnetic structure is indicated by filled (open) symbols for the Co atoms. These symbols represent equal (opposite) moment direction.

III. X-RAY AND NEUTRON-DIFFRACTION RESULTS

A. Crystallographic structure

Structurally, the parent compound of $BaCo_{0.9}Ni_{0.1}S_{1.8}$ is $BaNiS_2$, a tetragonal compound[2] with space group *P4/nmm* (No. 129) with lattice constants $a = 4.559$ Å, $c = 8.990$ Å. Nickel atoms are coordinated to five sulfur atoms, situated on the corners of a pyramid. The apycal sulfurs alternate below and above the plane formed by the edge-sharing pyramids. This configuration leads to Ni-S bonds pointing alternatingly up and down from the plane, which can also be envisaged as a double-layer of Ni atoms where nearest-neighbor (NN) nickels are in a different z plane, but next-nearest-neighbor (NNN) nickel atoms lie in the same z plane. In contrast to $BaNiS_2$, $BaCoS_2$ crystallizes in an orthorhombic structure (space group *Cmma*, No. 67), with lattice parameters $a \sim b \sim \sqrt{2}\,a$ ($BaNiS_2$) and $c \sim c(BaNiS_2)$. For intermediate concentrations in the mixed system $BaCo_{1-x}Ni_xS_{2-y}$ the tetragonal structure is stable for $x = 0.1$, the composition being studied here.

Figure 1 displays the crystal structure of $BaCo_{0.9}Ni_{0.1}S_{1.8}$. The low-temperature orthorhombic distortion is too small to visualize. The cobalt and nickel atoms are clearly visible inside a pyramid of sulfur atoms, forming a double layer, with the separation between the two Co/Ni monolayers equalling $\sim 0.18c$. Refinement of our x-ray diffractogram at room temperature, assuming the tetragonal $BaNiS_2$ structure, shows the presence of approximately 3.3 vol % of the second phase Ba_2CoS_3. This however will not influence our following discussion. Table I contains the

TABLE I. Structural and magnetic parameters for $BaCo_{0.9}Ni_{0.1}S_{1.8}$ at 287 and 19.4 K. T_N and the ordered cobalt moment are also indicated.

T (K)	a (Å)	b (Å)	c (Å)	Symmetry/moment
287	4.527	$b = a$	8.942	$P4/nmm$
19.4	6.355	6.448	8.901	$Cmma$
280 (T_N)	6.407	$b = a$	8.939	$1.8 \pm 0.5\ \mu_B$/Co

lattice constants derived from this refinement. The unit-cell lattice parameters in the tetragonal phase at 287 K are $a = 4.527$ Å, $c = 8.942$ Å, in good agreement with literature values. In Fig. 1 the a axis refers to the orthorhombic unit cell, i.e., $a_{\text{orth}} = \sqrt{2}a_{\text{tetr}}$. The reliability factor of the refinement, defined as $R_p = (\Sigma|I_m - I_c|)/\Sigma I_m$, equals $R_p = 2.7\%$. We have assumed random occupation of cobalt, nickel, and sulfur over their available positions. Due to the limited 2Θ range in our x-ray measurements, we could not perform a detailed refinement of the low-temperature crystal structure. Only the temperature dependence of the lattice parameters has been determined, thereby assuming the $BaCoS_2$-like orthorhombic structure. The c axis decreases linearly with decreasing temperature, from $c = 8.942$ Å at 287 K to 8.901 Å at 19.4 K (not shown). Any discontinuity at T_s is within the experimental uncertainty. Figure 2 shows the a and b lattice constants of the orthorhombic crystal structure, upon heating and cooling through T_s. The lattice constant in the tetragonal phase should be divided by $\sqrt{2}$ to obtain the unit-cell lattice constants. The lattice distortion results in a small splitting of the tetragonal (1 1 0) nuclear reflection. The inset of Fig. 2 shows the combined tetragonal (1 1 0) and (1 0 2) Bragg peaks at 287 K, and the strong broadening of the peak at lower angles at 19.4 K. In orthorhombic notation, these peaks at low T are the (2 0 0), (0 2 0), and (1 1 2) reflections. The broad peak can be fitted

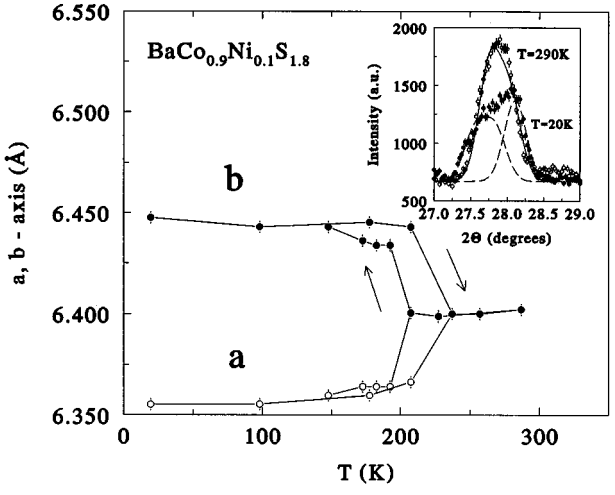

FIG. 2. The orthorhombic distortion of $BaCo_{0.9}Ni_{0.1}S_{1.8}$, displayed as the temperature dependence of the lattice parameters a and b. To obtain the unit-cell lattice constants in the tetragonal phase, above T_s, $a = b$ should be divided by $\sqrt{2}$. The inset shows the (1 1 0) and (1 0 2) reflection, indexed in the tetragonal lattice at 287 and 19.4 K. At 19.4 K, the broad peak at lower angles indicates splitting of the orhtorhombic (2 0 0) and (0 2 0) reflections.

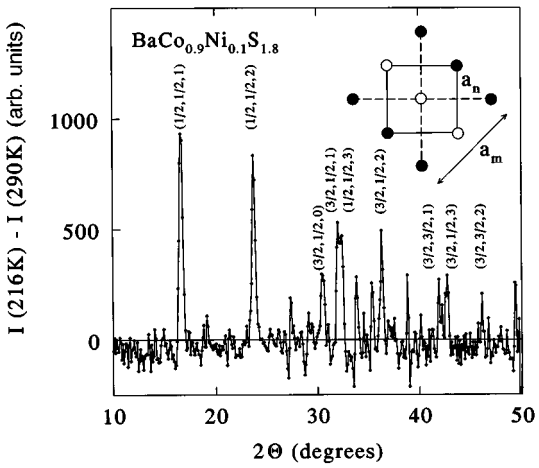

FIG. 3. Magnetic neutron intensity, derived from I(216 K)–I(290 K). The inset schematically pictures the AF structure of $BaCo_{0.9}Ni_{0.1}S_{1.8}$, showing only the Co/Ni positions in a double layer, projected onto the ab plane. The atoms connected by the solid lines and the dashed lines differ in height by $0.18c$. The magnetic lattice parameter $a_m = \sqrt{2}a_n$. Filled (open) symbols indicate equal (opposite) moment direction. The Co moments are likely oriented in the basal plane (see text).

to two Gaussians of equal width. We have not observed reflections of the type $(h\ k\ l/n)$ where n is an integer, which would indicate the formation of a superlattice as found in single-crystal diffraction.[4] Our data cannot distinguish between the $BaCoS_2$-type orthorhombic crystal structure, or small monoclinic distortions thereof. A definitive structure determination can best be performed on single-crystalline samples.

B. Magnetic structure

We have studied the magnetic structure by powder neutron diffraction on a different sample than used for the x-ray measurements. Refinement of the nuclear structure showed about 10 vol % of the parasitic Ba_2CoS_3 phase in this sample. A structure refinement of the diffractogram taken at 4.7 K, using the orthorhombic $BaCoS_2$ structure gave R factors of about 11%. Because of this large uncertainty in the determination of the nuclear structure, we focus on the magnetic properties of our sample. Figure 3 presents the difference spectrum, at low angles, between the diffractograms recorded at 216 K, where the magnetic intensity was strongest, and 290 K. For comparison, the strongest nuclear peak intensity is 2330 counts. Below 280 K, nine additional reflections are observed with indices $(h/2\ k/2\ l)$ with h, k odd. These can be indexed in a two times larger, tetragonal, magnetic lattice, rotated by 45° in the basal plane with lattice parameters $a_{\text{mag}} = \sqrt{2}\,a$ and $c_{\text{mag}} = c$. At 216 K, $a_{\text{mag}} = 6.407$ Å, and $c_{\text{mag}} = 8.939$ Å. In this setting, the magnetic ordering wave vector is $Q = (0\ 0\ 1)$. In the following discussion, we will use indices referring to the tetragonal nuclear structure. In Fig. 1 the magnetic structure is presented by filled (open) symbols for the cobalt atoms, representing equal (opposite) moment direction. The inset of Fig. 3 shows a projection of the magnetic structure onto the basal plane. Note that within a monolayer, the NN interaction is

TABLE II. Measured magnetic reflections and their integrated intensities at 216 K, compared with those calculated for the cobalt moment oriented along the *c* axis and in the basal plane. Our powder experiment does not allow determination of the moment direction (see text).

2Θ (deg)	$(h\ k\ l)$	I_{meas} (a.u.)	I_{calc} $\mu \parallel [001]$	I_{calc} $\mu \parallel [110]$
16.63	$\frac{1}{2}\ \frac{1}{2}\ 1$	100	100	67.2
23.75	$\frac{1}{2}\ \frac{1}{2}\ 2$	74.7	21.1	100
30.50	$\frac{3}{2}\ \frac{1}{2}\ 0$	28.6	16.7	7.1
31.99	$\frac{3}{2}\ \frac{1}{2}\ 1$	48.8	69.5	11.0
32.42	$\frac{1}{2}\ \frac{1}{2}\ 3$	42.5	5.9	55.9
36.35	$\frac{3}{2}\ \frac{1}{2}\ 2$	39.9	7.5	3.6
42.08	$\frac{3}{2}\ \frac{3}{2}\ 1$	22.3	7.3	4.7
42.72	$\frac{3}{2}\ \frac{1}{2}\ 3$	23.0	0.5	0.5
45.90	$\frac{3}{2}\ \frac{3}{2}\ 2$	13.0	12.0	11.9

antiferromagnetic. The orientation of Co moments between monolayers varies, being AF along one basal plane direction, and FM along the other.

The magnetic neutron intensities observed at 216 K are given in Table II. The powder nature of the experiment and the absence of $(\frac{1}{2}\ \frac{1}{2}\ 0)$ and $(0\ 0\ 1)$ magnetic reflections prohibit us from unambiguously establishing the moment direction in the ordered phase. However, the relatively strong $(\frac{1}{2}\ \frac{1}{2}\ 2)$ and $(\frac{1}{2}\ \frac{1}{2}\ 3)$ reflections as compared to $(\frac{1}{2}\ \frac{1}{2}\ 1)$ suggest that the moments lie in the basal plane, pointing along the NN direction $[1\ 1\ 0]$, since neutrons are only sensitive to spin components perpendicular to the scattering vector. Refinement of *all* magnetic reflections, however, gives equal fit quality for moments aligned along the *c* direction. The ordered cobalt moment was calculated by comparing the integrated intensities of all observed magnetic Bragg peaks with the nuclear $(0\ 0\ 1)$, $(1\ 1\ 2)$, and $(2\ 0\ 0)$ reflections. We have used the reported magnetic form factor.[9] This procedure yields an average cobalt moment of $\mu_{ord} = 1.8 \pm 0.5\mu_B$. A detailed neutron-diffraction study on single-crystal samples is necessary to completely describe the antiferromagnetic state. The magnetic structure is in accord with that observed recently by Kodama *et al.*[10] for stoichiometric $BaCoS_2$ and doped $BaCo_{0.825}Ni_{0.175}S_2$. This doped material has a similar ordered moment of $1.7\mu_B$ at 100 K.[10]

We have followed the temperature dependence of the magnetic intensity down to 4.7 K. Figure 4 displays the T dependence of the integrated intensities of the two strongest magnetic reflections, $(\frac{1}{2}\ \frac{1}{2}\ 1)$ and $(\frac{1}{2}\ \frac{1}{2}\ 2)$. The intensities are seen to monotonously increase below $T_N = 280 \pm 2$ K, reaching a maximum just above the AFI-PMM transition. Through this transition, the intensity drops by roughly a factor of 4. It follows closely the hysteresis in the structural distortion shown above in the x-ray data. Therefore, we believe that the residual antiferromagnetic intensity at 4.7 K is due to parts of the sample, with slightly different stoichiometry, that have not been transformed into the low-temperature crystal structure.[10] The amount of parasitic phase present in this sample may be an indication of such off-stoichiometry in the main phase. Our data are in conflict with recent observations by Felner *et al.*,[8] who claimed a persisting AF order in the metallic phase from their Mössbauer experiments. Mixed-phase material or sample inhomogeneity may explain such observations.

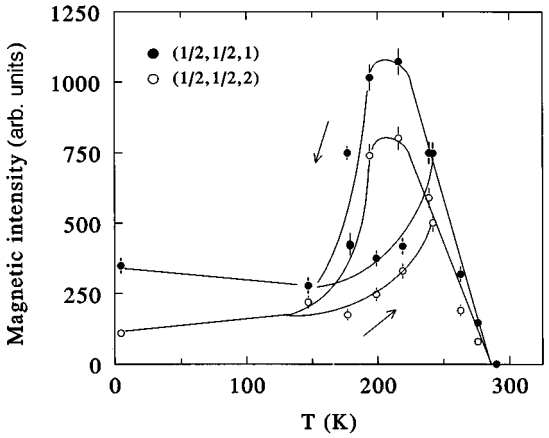

FIG. 4. The temperature dependence of the integrated intensity of the magnetic $(\frac{1}{2}\ \frac{1}{2}\ 1)$ and $(\frac{1}{2}\ \frac{1}{2}\ 2)$ Bragg peaks. T_N equals 280 ± 2 K. Note the small residual magnetic intensity below $T_s = 150$ K. This is attributed to incomplete phase transformation in our sample. The lines are a guide to the eye.

IV. ELECTRONIC PROPERTIES AND DILATOMETRY

A. Resistivity and thermoelectric power

The temperature dependence of the resistivity, $\rho(T)$, of a $BaCo_{1-x}Ni_xS_{2-y}$ sample with the nominal composition $x = 0.1$ and $y = 0.2$, sintered at 890 °C, is shown in Fig. 5(a). For this sample the temperature range of the hysteresis loop and the resistivity jump at T_s (two orders of magnitude upon cooling) are similar to those for the sample with $y = 0.15$ in Ref. 1. The conductivity of our samples in the AF phase is of order $1\text{–}10\ \Omega^{-1}\text{cm}^{-1}$, orders of magnitude smaller than Mott's minimal metallic conductivity, and comparable to that of the Mott insulator $BaCoS_2$ in the same range of temperatures. For $T > T_s$ the semilogarithmic graph of ρ vs T is a nearly straight line, $\ln(\rho/\rho_0) \propto -T$ (not shown). For more detail, we present the logarithmic derivative of ρ with respect to $1/T$, $d\ln\rho/d(1/T) = \Delta_l/k_B$, vs $1/T$ in Fig. 6. We find that Δ_l, known as the *local activation energy*, is *not* temperature independent as would be expected for a thermally activated process with a constant activation energy, Δ_a. Instead, it rises up to T_N. Over a wide temperature range it varies as T^2, and at a faster rate as T_N is approached. At the magnetic transition, it peaks and subsequently drops to a lower value. Although the T dependence of Δ_l varies for samples from different batches, the cusp at T_N is evident in all samples (as seen in the lower plot in Fig. 6 for a sample sintered at 850 °C). Close inspection of Fig. 3 of Ref. 5 shows that, for the compound $BaCoS_2$ below ~ 220 K, $\ln(\rho/\rho_0) \propto -T$ with Δ_l roughly two times larger than for our samples; in both cases $\Delta_l(T)$ follows the gradual drop of the susceptibility with decreasing T below T_N.[11]

From the relation between the local activation energy and Δ_a,

$$\Delta_l = \Delta_a - T\left(\frac{d\Delta_a}{dT}\right), \tag{1}$$

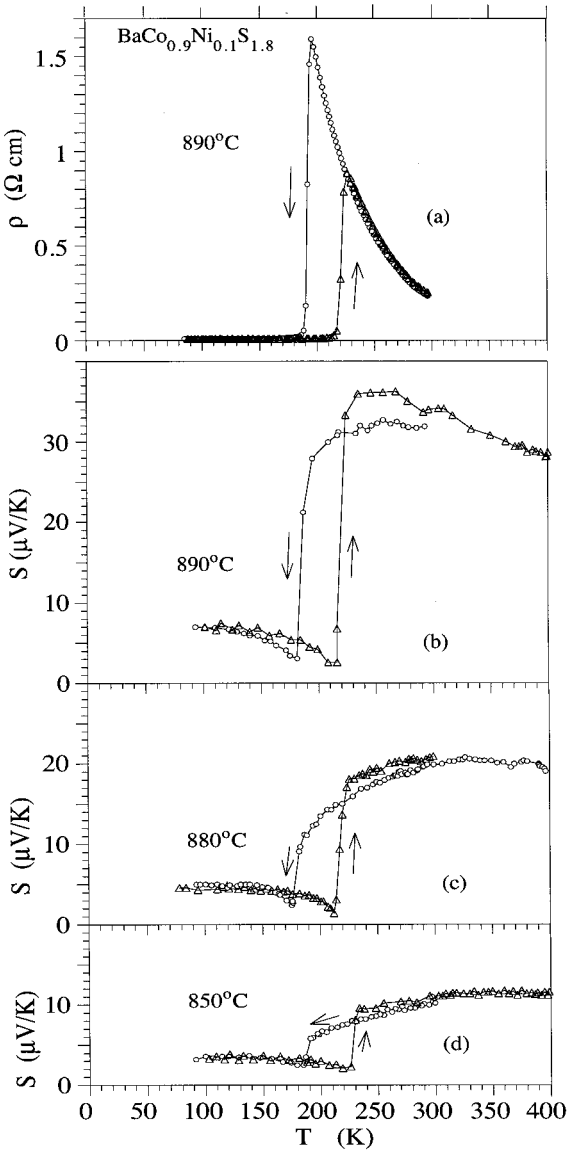

FIG. 5. Temperature dependence of the resistivity, $\rho(T)$, of a $BaCo_{0.9}Ni_{0.1}S_{1.8}$ sintered at 890 °C (a) and of the absolute thermopower, $S(T)$, of samples sintered at 890 °C (b), 880 °C (c) and 850 °C (d). The composition of the samples expressed in the formula is nominal.

the rise in Δ_l can be viewed as a result from a rapid decrease of the activation energy Δ_a with increasing T towards T_N, associated with, e.g., the closing of a gap as T_N is approached from below; in this regime $\Delta_l > \Delta_a$. In the temperature range where $\Delta_l \propto T^2$, observed for both our 890° sample and $BaCoS_2$, the drop of the activation energy with T may be approximated, by $\Delta_a \propto T(1-T/T_0)$, with T_0 a constant.

Figure 6 shows that T_N for the 850 °C sample is ~ 5 K lower than that for the 890 °C sample. The smaller resistivity jump and lower T_N both indicate a lower y/x ratio in this sample. By resistivity measurements only, it is impossible to distinguish between carrier excitations over a gap and nearest-neighbor hopping (NNH) in a band of localized states of width W ($\Delta_a \sim W/2$).[12,13] The negative temperature coefficient of ρ persists in the narrow temperature range between T_N and RT, with $\Delta_l \simeq 0.11$ and 0.08 eV for the 890 and 850 °C samples, respectively. This indicates that Δ_l above T_N and at least part of it below T_N is associated with NNH.

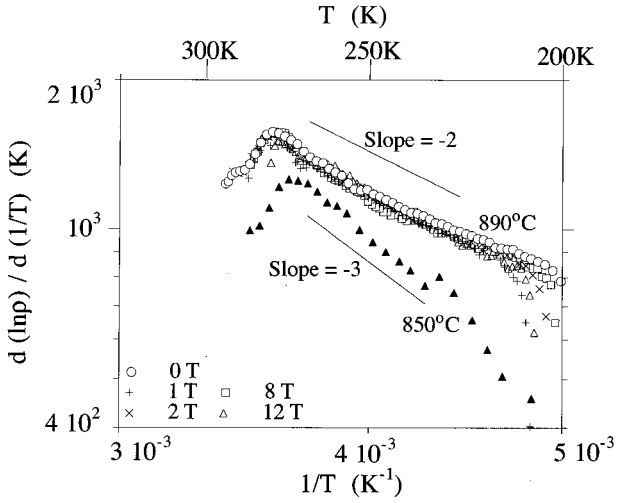

FIG. 6. Double-logarithmic graph of the local activation energy (in Kelvin) versus $1/T$ for various samples of $BaCo_{0.9}Ni_{0.1}S_{1.8}$, obtained from measurements in different magnetic fields. The sintering temperatures of the samples are indicated in the figure.

The absolute thermoelectric power (TEP), $S(T)$, is a very sensitive probe of the electronic structure of conductors around E_F, and particularly powerful in studying conductors with narrow bands and/or localized states. Figures 5(b)–5(d) display the temperature dependence of $-S(T)$ for samples with the same nominal composition ($x = 0.1$, $y = 0.2$) sintered at 890, 880, and 850 °C. As shown by the arrows, the TEP was measured while the samples were slowly cooled from RT down to 77 K and then slowly heated to 400 K. $S(T)$ is positive in the entire temperature range. The phase transition at T_s is marked by sharp jumps and hysteresis following those of $\rho(T)$. For $T > T_s^u$ (the upper transition temperature upon heating; the transition temperature upon cooling is labeled T_s^d) we observe differences between the results obtained upon cooling and heating, analogous to the findings from resistivity. The reproducibility is better in the 850 °C sample with the lower S. The AF transition temperature T_N is marked by a small decrease of $S(T)$ for the 890 °C sample. The rather small values of S above T_s favor electronic transport via hopping in a band of localized states in the whole temperature range. The possibility of excitations across a gap seems remote. To obtain such low $S(T)$ values, this process requires a high degree of electron-hole compensation, which is unlikely to occur in these rather heavily doped materials.

The thermoelectric power is defined as

$$S = \frac{1}{|e|T}\langle \mu - E \rangle, \tag{2}$$

where $\langle E-\mu \rangle$ is the average energy of the states participating in transport, measured from the chemical potential $-\mu$. Our results show that up to RT, $ST|e|/k_B = \langle \mu - E \rangle / k_B$ is one order of magnitude smaller than Δ_l, which either indi-

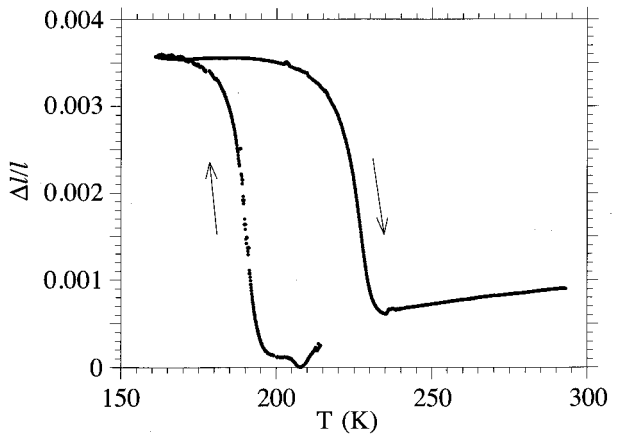

FIG. 7. Measured length changes of $BaCo_{0.9}Ni_{0.1}S_{1.8}$ versus temperature. Note the huge anomalies at T_s.

cates that the chemical potential is close to the middle of the band, or that $W \ll \Delta_l$ (i.e., W continues to decrease above T_N). TEP measurements above RT, recorded up to 400 K, further clarify the situation. Above T_s^u, $S(T)$ for the 890°C sample *decreases*, and those for the 880 and 850°C samples *increase*, towards saturation values. In the latter two samples $S(T)$ saturates near 300 K. A constant thermoelectric power is the most direct evidence for transport in a narrow band, i.e., $W \leqslant k_B T$. Below the AFI-PMM transition at T_s, S first rises with decreasing temperature, reaching constant values (or local maxima) around 100 K. The larger $S(400\,\mathrm{K})$ is accompanied by the larger $S(100\,\mathrm{K})$. For stoichiometric $BaCo_{1-x}Ni_xS_2$ and $0.2 \leqslant x \leqslant 0.6$, S has values in the $\mu V/K$ range, being positive at high temperatures and negative at low temperatures.[7] The small *positive* values of S in our metallic samples show that the sulfur vacancies shift the chemical potential upwards by filling holes in the band. We can therefore correlate the increase of the hole filling with an increase of the observed resistivity jump.

B. Magnetoresistance

Since magnetic ordering vanishes at T_s it is of interest to investigate the role of large applied magnetic fields on the phase transition. Figure 5(a) presents ρ vs T in zero field, while Fig. 6 shows double logarithmic graphs of Δ_l/k_B vs $1/T$ for various values of magnetic fields up to 12 T from 200 to 300 K. The effect of high magnetic fields on the resistivity is negligible both above and below the antiferromagnetic transition. A field of 12 T shifts T_N slightly towards lower temperatures. The structural transition is unaffected by a magnetic field (not shown). The observed small shifts of T_s^d and T_s^u by up to 3 K may be attributed to differences in the cooling or heating rates in the different cycles.

C. Dilatometry

The measured length changes of several samples as a function of temperature are presented in Fig. 7. Data were recorded upon changing temperature by about 1 K/min. The phase transition at T_s is accompanied by a contraction on heating and corresponding expansion on cooling; the relative change of length is $\Delta l/l = (3.5 \pm 0.5) \times 10^{-3}$, both on heating and cooling. The hysteresis is clearly visible: on cooling the transition takes place at $T_s^d = 189 \pm 2$ K, on heating at $T_s^u = 221 \pm 2$ K. We find that 90% of the transition takes place within about 15 K. The hysteresis loop widens (narrows) if higher (lower) heating or cooling rates are employed. It is surprising that in spite of the large distortions and strains which this phase transition must cause in the polycrystalline material, the sample does not desintegrate. However the length changes vary slightly from run to run, probably due to slight attrition during temperature cycling. The observed length change is about one to two orders of magnitude larger than those accompanying usual phase transitions. The transition temperature and $\Delta l/l$ depend slightly on the sintering temperature of the sample. For $T_{\mathrm{sinter}} = 850\,^{\circ}\mathrm{C}$ we find $T_s^u = 220$ K, while for $T_{\mathrm{sinter}} = 890\,^{\circ}\mathrm{C}$ $T_s^u = 225$ K. Assuming an isotropic, polycrystalline sample, we calculate a volume change of $\Delta V/V = 3\Delta l/l = (1.05 \pm 0.15) \times 10^{-2}$. This is in fair agreement with the value of $\Delta V/V = 0.01$ reported by Looney *et al.*,[4] but larger than observed in our x-ray experiment ($\Delta V/V = 0.004$). These different results indicate the presence of significant sample dependences in the structural changes at T_s.

V. SUMMARY

We have investigated the crystal and magnetic structure of the layered sulfide $BaCo_{0.9}Ni_{0.1}S_{1.8}$, which displays an antiferromagnetic transition at 280 K, followed by an insulator to metal transition that is accompanied by a lowering of the crystal symmetry from tetragonal to, within our resolution, orthorhombic at 200 K. The latter transition exhibits large hysteresis, and results in the loss of long-range antiferromagnetic order. From resistivity we have derived the temperature dependence of the local activation energy, and propose nearest-neighbor hopping in a band of localized states as the dominant mechanism for electronic transport. This conclusion is supported by the observation of saturation of the thermoelectric power near 300 K. Large magnetic fields up to 12 T do not significantly influence either magnetic or structural phase transition.

The measured properties of $BaCo_{0.9}Ni_{0.1}S_{1.8}$ are found to be sensitive to the exact preparation conditions. In future experimental studies, better control of the stoichiometry and thereby of the band filling (suggested to govern the size of the resistivity jump at T_s) is needed. Further neutron scattering on single crystals[14] should be performed to establish the magnetic moment direction and investigate the dynamics associated with the structural phase transition. Single crystals are also needed for studying the anisotropy of magnetic and transport properties, given the two-dimensional character of this interesting alloy system.

ACKNOWLEDGMENTS

We thank R. L. Donaberger and I. P. Swainson of Chalk River Laboratories and J. W. L. Pang for technical assistance. This research was partially supported by the Canadian Institute for Advanced Research and the Natural Sciences and Engineering Research Council of Canada. The research of the Technion group was supported by the Israel Science Foundation administered by the Israel Academy of Sciences and Humanities, and by the Fund for the Promotion of Research at Technion.

[*]Present address: Philips Research Laboratories, Prof. Holstlaan 4, 5656 AA Eindhoven, The Netherlands.

[1] L.S. Martinson, J.W. Schweitzer, and N.C. Baenziger, Phys. Rev. Lett. **71**, 125 (1993).

[2] L.E. Grey and H. Steinfink, J. Am. Chem. Soc. **92**, 5093 (1970).

[3] J.C. Phillips, Phys. Rev. B **47**, 11 615 (1993); Phys. Rev. Lett. **72**, 3863 (1994).

[4] C. Looney, J.S. Schilling, L.S. Martinson, and J.W. Schweitzer, Phys. Rev. Lett. **76**, 4789 (1996).

[5] G.J. Snyder, M.C. Gelabert, and F.J. DiSalvo, J. Solid State Chem. **113**, 355 (1994).

[6] N.C. Baenziger, L. Grout, L.S. Martinson, and J.W. Schweitzer, Acta Crystallogr. C **50**, 1375 (1994).

[7] J. Takeda, K. Kodama, H. Harashina, and M. Sato, J. Phys. Soc. Jpn. **63**, 3564 (1994).

[8] I. Felner, J. Gersten, S. Litvin, U. Asaf, and T. Kröner, Phys. Rev. B **52**, 10 097 (1995).

[9] R.M. Moon, Phys. Rev. **136**, A195 (1964).

[10] K. Kodama, S. Shamoto, H. Harashina, J. Takeda, M. Sato, K. Kakurai, and M. Nishi, J. Phys. Soc. Jpn. **65**, 1782 (1996).

[11] $\chi(T)$ is shown in Fig. 4 of Ref. 5 for $BaCoS_2$ and in Fig. 3 of Ref. 1 for $BaCo_{0.9}Ni_{0.1}S_{2-y}$.

[12] N.F. Mott and E.A. Davis, *Electronic Processes in Noncrystalline Materials* (Clarendon, Oxford, 1979).

[13] B.I. Shklovskii and A.L. Efros, *Electronic Properties of Doped Semiconductors* (Springer-Verlag, Berlin, 1984).

[14] S. Shamoto, S. Tanaka, E. Ueda, and M. Sato, Physica C **263**, 550 (1996).